

Supporting information for

**Temperature- and pressure-induced phase transitions in niccolite-type formate framework of
[H₃N(CH₃)₄NH₃][Mn₂(HCOO)₆]**

*Mirosław Maczka,^{*a} Anna Gągor,^a Nathalia Leal Marinho Costa,^b Waldeci Paraguassu,^b Adam Sieradzki,^c and Adam Pikul^a*

^a*Institute of Low Temperature and Structure Research, Polish Academy of Sciences, Box 1410, 50-950 Wrocław 2, Poland*

^b*Faculdade de Física, Universidade Federal do Pará, 66075-110, Belém, PA, Brazil*

^c*Department of Experimental Physics, Wrocław University of Technology, Wybrzeże Wyspiańskiego 27, 50-370, Wrocław, Poland*

*e-mail: m.maczka@int.pan.wroc.pl

Table S1. Experimental details.

For all structures: $C_{10}H_{20}Mn_2N_2O_{12}$, $M_r = 470.16$. Experiments were carried out with Mo $K\alpha$ radiation. H-atom parameters were constrained. Empirical absorption correction using spherical harmonics, implemented in SCALE3 ABSPACK scaling algorithm was used.

Crystal system, space group	Trigonal, $P-31c$	Monoclinic, Cc	Monoclinic, Cc	Monoclinic, Cc	Monoclinic, Cc
Temperature (K)	360	345	298	160	90
a, b, c (Å)	8.6962 (2), 8.6962 (2), 13.5672 (6)	8.5685 (2), 15.3292 (4), 13.6602 (3)	8.5608 (2), 15.3339 (3), 13.6433 (3)	8.5542 (2), 15.2990 (3), 13.6149 (3)	8.5477 (2), 15.2820 (3), 13.6085 (3)
α, β, γ (°)	90, 90, 120	90, 90.226 (2), 90	90, 90.190 (2), 90	90, 90.100 (2), 90	90, 90.060 (2), 90
V (Å ³), Z	894.44 (6), 2	1794.24 (8), 4	1790.95 (7), 4	1781.79 (7), 4	1777.61 (7), 4
μ (mm ⁻¹)	1.475	1.470	1.473	1.481	1.484
Crystal size (mm)	0.21 × 0.18 × 0.17	0.21 × 0.18 × 0.17	0.21 × 0.18 × 0.17	0.20 × 0.18 × 0.16	0.20 × 0.18 × 0.16
T_{\min}, T_{\max}	0.846, 1.000	0.965, 1.000	0.863, 1.000	0.897, 1.000	0.909, 1.000
No. of measured, independent and observed [$I > 2\sigma(I)$] reflections	9753, 739, 675	8647, 2751, 2323	9298, 3788, 3599	10639, 3880, 3596	10570, 3860, 3638
Diffractometer	Sapphire1,	Sapphire1,	Sapphire1,	Atlas	Atlas
R_{int}	0.023	0.035	0.018	0.030	0.038
(sin θ/λ) _{max} (Å ⁻¹)	0.665	0.610	0.667	0.694	0.694
$R[F^2 > 2\sigma(F^2)], wR(F^2), S$	0.048, 0.139, 1.2	0.031, 0.067, 0.98	0.033, 0.084, 1.10	0.026, 0.060, 1.04	0.026, 0.055, 1.03
No. of reflections	739	2751	3788	3880	3860
No. of parameters	44	246	239	239	239
No. of restraints	3	14	10	10	10
$\Delta\rho_{\max}, \Delta\rho_{\min}$ (e Å ⁻³)	0.91, -0.58	0.34, -0.35	1.69, -0.49	0.74, -0.28	0.29, -0.31
Absolute structure	—		Refined as an inversion twin.		
Absolute structure parameter	—	0.38 (5)	0.34 (2)	0.41 (2)	0.404 (19)

Computer programs: *CrysAlis PRO*, Agilent Technologies, Version 1.171.37.35h. *CrysAlis PRO* 1.171.38.41 (Rigaku OD, 2015), *SHELXL2014/7*

Table S2. Selected geometric parameters (Å)

	(360K)	(345K)	(298K)		
Mn1—O1 ⁱ	2.174 (3)	Mn1—O5	2.138 (8)	Mn1—O5	2.140 (3)
Mn1—O1 ⁱⁱ	2.174 (3)	Mn1—O3	2.182 (5)	Mn1—O6	2.169 (2)
Mn1—O1 ⁱⁱⁱ	2.174 (3)	Mn1—O6	2.166 (7)	Mn1—O3	2.177 (2)
Mn1—O1 ^{iv}	2.174 (3)	Mn1—O2	2.195 (5)	Mn1—O2	2.193 (2)
Mn1—O1 ^v	2.174 (3)	Mn1—O4	2.198 (6)	Mn1—O1	2.192 (2)
Mn1—O1	2.174 (3)	Mn1—O1	2.194 (6)	Mn1—O4	2.207 (2)
Mn2—O2	2.173 (2)	Mn2—O11	2.141 (6)	Mn2—O11	2.140 (3)
Mn2—O2 ^{vi}	2.173 (2)	Mn2—O8	2.165 (6)	Mn2—O8	2.162 (2)
Mn2—O2 ^{vii}	2.173 (2)	Mn2—O7	2.161 (6)	Mn2—O9	2.166 (2)
Mn2—O2 ^{viii}	2.173 (2)	Mn2—O9	2.174 (6)	Mn2—O7	2.178 (3)
Mn2—O2 ^{ix}	2.173 (2)	Mn2—O10	2.198 (6)	Mn2—O12	2.199 (2)
Mn2—O2 ^x	2.173 (2)	Mn2—O12	2.198 (5)	Mn2—O10	2.205 (2)
C1—O1	1.225 (4)	O1—C6	1.225 (10)	O1—C6	1.242 (4)
C1—O2	1.229 (4)	O2—C5	1.266 (10)	O2—C5	1.259 (4)
N1—C2	1.4484 (10)	O3—C1	1.258 (10)	O3—C1	1.250 (4)
C2—C3	1.499 (8)	O4—C2	1.229 (9)	O4—C2	1.235 (4)
C3—C3 ^v	1.445 (9)	O5—C4	1.214 (11)	O5—C4	1.227 (4)
		O6—C3	1.235 (10)	O6—C3	1.224 (4)
		O7—C5 ^{xi}	1.249 (9)	O7—C5 ⁱ	1.244 (4)
		O8—C1	1.235 (10)	O8—C1	1.236 (4)
		O9—C6 ^{xii}	1.219 (9)	O9—C6 ⁱⁱ	1.232 (4)
		O10—C2 ^{xiii}	1.231 (10)	O10—C2 ⁱⁱⁱ	1.233 (4)
		O11—C4 ^{xiv}	1.201 (11)	O11—C4 ^{iv}	1.217 (4)
		O12—C3 ^{xv}	1.248 (10)	O12—C3 ^v	1.248 (4)
		C2—O10 ^{xvi}	1.231 (10)	C2—O10 ^{vi}	1.233 (4)
		C3—O12 ^{xvii}	1.248 (10)	C3—O12 ^{vii}	1.248 (4)
		C4—O11 ^{xviii}	1.201 (11)	C4—O11 ^{viii}	1.217 (4)
		C5—O7 ^{xix}	1.249 (9)	C5—O7 ^{ix}	1.244 (4)
		C6—O9 ^{xx}	1.219 (9)	C6—O9 ^x	1.232 (4)
		N1—C14	1.475 (10)	C11—N2	1.479 (5)
		N2—C11	1.477 (9)	C11—C12	1.545 (6)
		C11—C12	1.521 (9)	C12—C13	1.474 (4)
		C12—C13	1.501 (6)	C13—C14	1.549 (6)
		C13—C14	1.561 (11)	C14—N1	1.483 (5)
		C15—C16	1.465 (13)		

(160K)	(90K)
Mn1—O5	2.136 (4)
Mn1—O6	2.172 (3)
Mn1—O3	2.176 (3)
Mn1—O2	2.191 (3)
Mn1—O1	2.191 (3)
Mn1—O4	2.203 (3)
Mn2—O11	2.146 (3)
Mn2—O8	2.163 (3)
Mn2—O9	2.167 (3)
Mn2—O7	2.177 (3)
Mn2—O10	2.192 (3)
Mn2—O12	2.202 (3)
O1—C6	1.251 (5)
O2—C5	1.266 (5)
O3—C1	1.251 (5)
O4—C2	1.248 (5)
Mn1—O5	2.138 (3)
Mn1—O6	2.170 (3)
Mn1—O3	2.173 (3)
Mn1—O1	2.187 (3)
Mn1—O2	2.192 (3)
Mn1—O4	2.202 (3)
Mn2—O11	2.148 (3)
Mn2—O8	2.159 (3)
Mn2—O9	2.170 (2)
Mn2—O7	2.176 (2)
Mn2—O10	2.190 (2)
Mn2—O12	2.203 (3)
O1—C6	1.257 (5)
O2—C5	1.267 (4)
O3—C1	1.264 (4)
O4—C2	1.255 (4)

O5—C4	1.240 (5)	O5—C4	1.237 (5)
O6—C3	1.238 (5)	O6—C3	1.246 (4)
O7—C5 ⁱ	1.250 (5)	O7—C5 ⁱ	1.254 (4)
O8—C1	1.248 (5)	O8—C1	1.250 (4)
O9—C6 ⁱⁱ	1.247 (5)	O9—C6 ⁱⁱ	1.248 (4)
O10—C2 ⁱⁱⁱ	1.250 (5)	O10—C2 ⁱⁱⁱ	1.255 (4)
O11—C4 ^{iv}	1.239 (5)	O11—C4 ^{iv}	1.251 (4)
C2—O10 ^v	1.250 (5)	O12—C3 ^v	1.255 (4)
C3—O12 ^{vi}	1.260 (5)	C2—O10 ^{vi}	1.255 (4)
C4—O11 ^{vii}	1.239 (5)	C3—O12 ^{vii}	1.255 (4)
C5—O7 ^{viii}	1.250 (5)	C4—O11 ^{viii}	1.251 (4)
C6—O9 ^{ix}	1.247 (5)	C5—O7 ^{ix}	1.254 (4)
C11—N2	1.493 (5)	C6—O9 ^x	1.248 (4)
C11—C12	1.530 (5)	C11—N2	1.496 (4)
C12—C13	1.503 (4)	C11—C12	1.523 (5)
C13—C14	1.535 (5)	C12—C13	1.515 (4)
C14—N1	1.498 (5)	C13—C14	1.528 (5)
O6—C3	1.238 (5)	C14—N1	1.494 (4)

Symmetry code(s): (i) $-y+1, -x+1, -z+1/2$; (ii) $x, x-y, -z+1/2$; (iii) $-x+y+1, -x+1, z$; (iv) $-y+1, x-y, z$; (v) $-x+y+1, y, -z+1/2$; (vi) $-x+2, -y, -z$; (vii) $x-y, x-1, -z$; (viii) $-x+y+2, -x+1, z$; (ix) $-y+1, x-y-1, z$; (x) $y+1, -x+y+1, -z$; (xi) $x+1/2, -y+3/2, z-1/2$; (xii) $x-1/2, y-1/2, z$; (xiii) $x, -y+1, z-1/2$; (xiv) $x-1/2, -y+3/2, z-1/2$; (xv) $x+1/2, y-1/2, z$; (xvi) $x, -y+1, z+1/2$; (xvii) $x-1/2, y+1/2, z$; (xviii) $x+1/2, -y+3/2, z+1/2$; (xix) $x-1/2, -y+3/2, z+1/2$; (xx) $x+1/2, y+1/2, z$.

Table S3. Selected hydrogen bond parameters.

$D-H\cdots A$	$D-H$ (Å)	$H\cdots A$ (Å)	$D\cdots A$ (Å)	$D-H\cdots A$ (°)
(345K)				
N1—H1A···O12 ⁱⁱ	0.89	2.02	2.863 (7)	156.9
N1—H1B···O4 ⁱⁱⁱ	0.89	2.26	3.138 (8)	170.6
N1—H1C···O3 ^{iv}	0.89	1.93	2.823 (8)	175.1
N2—H2A···O10 ^v	0.89	2.01	2.895 (9)	175.4
N2—H2B···O1	0.89	2.11	2.939 (8)	154.9
N2—H2C···O2 ^{vi}	0.89	2.03	2.912 (8)	170.5
(298K)				
N1—H1A···O12 ⁱ	0.89	2.03	2.855 (4)	153.2
N1—H1B···O4 ⁱⁱ	0.89	2.23	3.118 (4)	174.5
N1—H1C···O3 ⁱⁱⁱ	0.89	1.94	2.829 (4)	178.0
N2—H2A···O2 ^{iv}	0.89	2.04	2.925 (4)	172.2
N2—H2A···O7 ^v	0.89	2.59	3.171 (4)	123.5
N2—H2B···O10 ^{vi}	0.89	2.00	2.880 (4)	171.6
N2—H2C···O1	0.89	2.08	2.926 (4)	158.7
(160K)				
N1—H1A···O12 ⁱ	0.89	2.01	2.842 (4)	156.2
N1—H1B···O4 ⁱⁱ	0.89	2.18	3.065 (4)	172.1
N1—H1C···O3 ⁱⁱⁱ	0.89	1.93	2.820 (4)	175.5
N2—H2A···O2 ^{iv}	0.89	2.04	2.919 (4)	171.4
N2—H2A···O7 ^v	0.89	2.57	3.164 (4)	124.7
N2—H2B···O10 ^{vi}	0.89	1.99	2.868 (4)	170.9
N2—H2C···O1	0.89	2.05	2.900 (4)	159.4
(90K)				
N1—H1A···O12 ⁱ	0.89	2.00	2.843 (4)	158.7
N1—H1B···O4 ⁱⁱ	0.89	2.17	3.045 (3)	169.2
N1—H1C···O3 ⁱⁱⁱ	0.89	1.93	2.817 (3)	172.6
N2—H2A···O2 ^{iv}	0.89	2.03	2.908 (4)	171.3
N2—H2A···O7 ^v	0.89	2.57	3.160 (4)	124.9
N2—H2B···O10 ^{vi}	0.89	1.98	2.859 (3)	170.4
N2—H2C···O1	0.89	2.04	2.897 (4)	160.1

Symmetry code(s): (i) $x+1/2, -y+3/2, z+1/2$; (ii) $x, -y+1, z-1/2$; (iii) $x, y, z-1$; (iv) $x-1/2, -y+3/2, z-1/2$; (v) $x+1/2, y+1/2, z$; (vi) $x, -y+2, z-1/2$; (vii) $x-1/2, -y+3/2, z+1/2$; (viii) $x-1/2, y+1/2, z$.

Tables S4. The results of the mode analysis performed in AMPLIMODES.

WP		Atom	ux	uy	uz	u
4a	(x,y,z)	Mn1	-0.0013	0.0024	-0.0006	0.0390
4a	(x,y,z)	Mn2	0.0005	0.0020	0.0014	0.0366
4a	(x,y,z)	C1	0.0190	0.0050	0.0071	0.2067
4a	(x,y,z)	C1_2	0.0070	0.0209	-0.0127	0.3659
4a	(x,y,z)	C1_3	0.0053	0.0037	-0.0050	0.0997
4a	(x,y,z)	C1_4	-0.0086	-0.0003	0.0029	0.0850
4a	(x,y,z)	C1_5	-0.0083	-0.0011	-0.0073	0.1247
4a	(x,y,z)	C1_6	0.0018	-0.0126	-0.0118	0.2496
4a	(x,y,z)	O1	0.0109	0.0026	0.0032	0.1120
4a	(x,y,z)	O1_2	0.0046	-0.0045	0.0103	0.1613
4a	(x,y,z)	O1_3	0.0153	0.0037	-0.0134	0.2338
4a	(x,y,z)	O1_4	-0.0177	0.0043	-0.0113	0.2282
4a	(x,y,z)	O1_5	-0.0132	0.0040	-0.0032	0.1370
4a	(x,y,z)	O1_6	-0.0258	0.0019	0.0262	0.4249
4a	(x,y,z)	O2	0.0129	0.0044	0.0021	0.1336
4a	(x,y,z)	O2_2	0.0111	0.0013	0.0110	0.1801
4a	(x,y,z)	O2_3	0.0144	0.0051	-0.0098	0.1999
4a	(x,y,z)	O2_4	-0.0059	0.0024	0.0005	0.0630
4a	(x,y,z)	O2_5	-0.0110	0.0002	-0.0075	0.1412
4a	(x,y,z)	O2_6	-0.0110	0.0112	0.0182	0.3158

NOTE: ux, uy and uz are given in relative units. |u| is the absolute distance given in Å

Maximum atomic displacement in the distortion, Δ : 0.4249 Å

Total distortion amplitude: 1.2907 Å

Symmetry Modes Summary

Atoms	W P	Modes
O1, O2, C1	$12i$	GM1+(3), GM3+(6), GM2-(3), GM3-(6)
Mn1	$2d$	GM3+(1), GM2-(1), GM3-(1)
Mn2	$2b$	GM2-(1), GM3-(2)

Note: The primary mode is written in bold letters

Summary of Amplitudes

K-vector	Irrep	Direction	Isotropy subgroup		Dimension	Amplitude (Å)
(0,0,0)	GM1 +	(a)	P-31c	(163)	9	0.2152
(0,0,0)	GM3 +	(-0.500a,0.866a)	C2/c	(15)	19	1.0779
(0,0,0)	GM2-	(a)	P31c	(159)	11	0.3203
(0,0,0)	GM3-	(-0.866a,-0.500a)	Cc	(9)	21	0.5959

Global distortion: 1.2907 Å

Summary of AMPLIMODES analysis:

The structure of the monoclinic phase has four distortion modes of $P\bar{3}1c$, $C2/c$, $P31c$ and Cc symmetry. The two latter are polar, and the last one is a primary mode. The displacements of the metal ions have the symmetry of both polar modes, Cc and $P31c$, and give rise to the spontaneous polarization. The Mn^{2+} ions, on both lattice sites, have nearly the same shifts, equal to ~ 0.04 Å. The monoclinic distortion affects also the positions of oxygen and carbon atoms that were occupied in trigonal phase. All of them shift accordingly to four symmetry modes accompanying the $P\bar{3}1c$ to Cc symmetry reduction with a similar contribution of polar and non-polar modes. The maximum atomic displacement in the distortion concerns O(1) oxygen that shifts 0.4 Å. The calculations were done for ordered atoms: metal centers as well as oxygen and carbon atoms from the formate linkers. Similar analysis has also been done for $Mg_2[COOH]_6^{2-}$ framework basing on the data from Ref. 1 for comparison. The total distortion amplitude that is given by the square root of the sum of the squares of all atomic displacements is equal to 1.3 Å for $Mn_2[COOH]_3^{2-}$ and is only slightly higher from the global distortion of the $Mg_2[COOH]_3^{2-}$ framework which amounts to 1.2 Å. In both compounds, the total amplitude of the polar primary mode equals 0.6 Å, whereas the amplitude of the strongest secondary mode (of $C2/c$ symmetry) amounts to nearly 1.1 Å showing a comparable contribution of the primary and secondary modes into distortion. Å.

[1] R. Shang, G.-C. Xu, Z.-M. Wang, S. Gao, *Chem. Eur. J.* 2014, **20**, 1146-1158.

Table S5. IR and Raman frequencies (in cm^{-1}) of bnMn and suggested assignments.^a

Raman 380 K	Raman 80 K	IR 410 K	IR 5 K	assignment
		3171sh	3161w, 3142m	$\nu(\text{NH}_3)$
		3066m,b	3098sh, 3073sh	$\nu(\text{NH}_3)$
			3062sh	
		3047w	3031m	$\nu(\text{NH}_3)$
		3022w	3013m	$\nu(\text{NH}_3)$
3004m	2997m	3001w	2998w	$\nu_{\text{as}}(\text{CH}_2)$
2968s	2967sh, 2962s	2969m	2970w	$\nu_{\text{as}}(\text{CH}_2)$
	2958sh			
	2942w	2945vw		$\nu_{\text{as}}(\text{CH}_2)$
		2940m,b	2950m	$\nu(\text{NH}_3)$
2938s	2931s			$\nu_{\text{as}}(\text{CH}_2)$
2912vw			2909w	overtone $\delta(\text{CH}_2)$
2893w	2898w, 2892w		2899w	$\nu_s(\text{CH}_2)$
2862sh	2861s		2872w, 2861w 2859w	$\nu_s(\text{CH}_2)$
2841s	2841s	2848sh, 2836m	2845sh, 2841m, 2839m, 2832m	$\nu_1(\text{HCOO}^-)$
			2818w	
		2779w,b	2793vw, 2785vw	overtones
			2772vw	
		2739vw	2749vw	overtones
		2721w	2731w	overtones
		2683vw,b	2700w	overtones
		2618vw,b	2645w	overtones

		2603w,b	2609w	overtones
			1667w, 1652vw	$\delta_{as}(NH_3)$
		1628sh	1629w	$\delta_{as}(NH_3)$
		1590s	1594s, 1582s	$\nu_4(HCOO^-)$
		1516w,b	1535m, 1530m	$\delta_s(NH_3)$
1454vw, 1439w	1461vw, 1437vw 1435w	1460vw, 1452w 1447w, 1435vw	1462w, 1453w, 1446w, 1435w	$\delta(CH_2)$
1374m	1391sh, 1375s	1386sh, 1376s	1388s, 1382s	$\nu_5(HCOO^-)$
	1368w		1376s	
1359s	1362s, 1352s	1359sh, 1350s	1368m, 1364s 1360w, 1353s	$\nu_2(HCOO^-)$
			1346s	
	1330vw, 1318vw		1317w, 1309w	$\omega(CH_2)$
			1284vw	$\tau(CH_2)$
		1262w,b	1264w, 1257sh	$\tau(CH_2)$
	1203vw		1203w	$\tau(CH_2)$
		1167w	1171w	$\rho(NH_3)$
		1104w	1114w	$\rho(NH_3)$
1066w	1072w	1070w	1082w, 1075w 1070w	$\nu_6(HCOO^-)$
		1050w		$\nu(CC)$
1027w		1025w	1032w, 1024vw	$\nu(CC)$
998w	1013w			$\nu(CC)$
	998vw	994w	998w	$\rho(NH_3)$
		902w,b	916w	$\rho(NH_3)$
871w	879w	876sh, 882w	880w, 888w	$\nu(CN)$

		841vw		overtone
790w, 787w	799w, 793w 787w	789s	807s, 801w	$\nu_3(\text{HCOO}^-)$
			797sh, 795s	
			790s, 785s	
		740w	739w	$\rho(\text{CH}_2)$
	516vw	518vw		$\delta(\text{CCC})$
			478w, 491w	$\delta(\text{CCC})$
		444w	451m	$\delta(\text{CCN})$
	277w			$\text{L}(\text{HCOO}^-)$ and $\text{T}'(\text{HCOO}^-)$
218m	248m, 228m			$\text{L}(\text{HCOO}^-)$
174s	210sh, 201w			$\text{L}(\text{HCOO}^-)$
	187m, 178m			
126s	161w, 144sh			$\text{L}(\text{HCOO}^-)$
	138m, 129w			
101m	112m, 98w, 87m			$\text{L}(\text{bnH}_2^{2+})$ and $\text{T}'(\text{bnH}_2^{2+})$

^aKey: s, strong; m, medium; w, weak; vw, very weak; sh, shoulder; b, broad; Internal vibrations of HCOO^- ions are classified as C-H stretching (ν_1), symmetric C-O stretching (ν_2), antisymmetric C-O stretching (ν_4), symmetric O-C-O bending (ν_3), C-H in-plane bending (ν_5) and C-H out-of-plane bending (ν_6) modes. Internal vibrations of bnH_2^{2+} cation are subdivided into symmetric stretching ($\nu_s(\text{CH}_2)$), antisymmetric stretching ($\nu_{as}(\text{CH}_2)$), scissoring ($\delta(\text{CH}_2)$), rocking ($\rho(\text{CH}_2)$), wagging ($\omega(\text{CH}_2)$) and torsion or twisting ($\tau(\text{CH}_2)$) modes of the CH_2 groups as well as symmetric stretching (ν_s), antisymmetric stretching (ν_{as}), bending (δ), rocking (ρ) and torsion (τ) modes of the NH_3 groups. The remaining vibrations correspond to CC and CN stretching as well as CCN in-plane bending and out-of-plane bending modes.

Table S6. Wavenumber intercepts at zero pressure (ω_0) and pressure coefficients ($\alpha=d\omega/dP$), obtained from fitting of the experimental data by linear functions, for the three phases of bnMn.

ambient pressure phase		Intermediate phase		high-pressure phase		assignment
ω_0	α	ω_0	α	ω_0	α	
(cm ⁻¹)	(cm ⁻¹ GPa ⁻¹)	(cm ⁻¹)	(cm ⁻¹ GPa ⁻¹)	(cm ⁻¹)	(cm ⁻¹ GPa ⁻¹)	
1372.3	3.6	1378.1	1.8	1380.3	1.0	$\nu_5(\text{HCOO}^-)$
1360.8	3.4	1363.6	1.0	1365.3	1.9	$\nu_2(\text{HCOO}^-)$
1350.5	8.3	1353.1	2.8	1360.1	0.5	$\nu_2(\text{HCOO}^-)$
1068.8	0.3	1066.8	4.2	1070.0	5.7	$\nu_6(\text{HCOO}^-)$
				1067.5	0.1	$\nu_6(\text{HCOO}^-)$
		1037.4	0.5	1048.1	-1.7	$\nu(\text{CC})$
1009.4	-0.6	1008.1	-2.2	1004.7	2.9	$\nu(\text{CC})$
				1001.2	-6.8	$\nu(\text{CC})$
876.3	1.5	875.4	2.4	882.8	0.8	$\nu(\text{CN})$
794.7	0.7	794.8	-1.0	784.2	3.2	$\nu_3(\text{HCOO}^-)$
784.8	1.7	786.9	0.1	776.2	-2.9	$\nu_3(\text{HCOO}^-)$
512.5	2.0	512.7	4.3	511.2	5.1	$\delta(\text{CCC})$
316.5	5.3			270.4	12.7	$\text{T}'(\text{HCOO}^-)$
219.5	6.7	227.3	10.9	250.1	0.4	$\text{L}(\text{HCOO}^-)$
				189.1	12.2	$\text{L}(\text{HCOO}^-)$
170.8	4.6	177.9	2.0	172.0	4.7	$\text{L}(\text{HCOO}^-)$
				177.3	-1.2	$\text{L}(\text{HCOO}^-)$
135.4	-7.3	137.7	-10.1	133.3	0.8	$\text{L}(\text{HCOO}^-)$

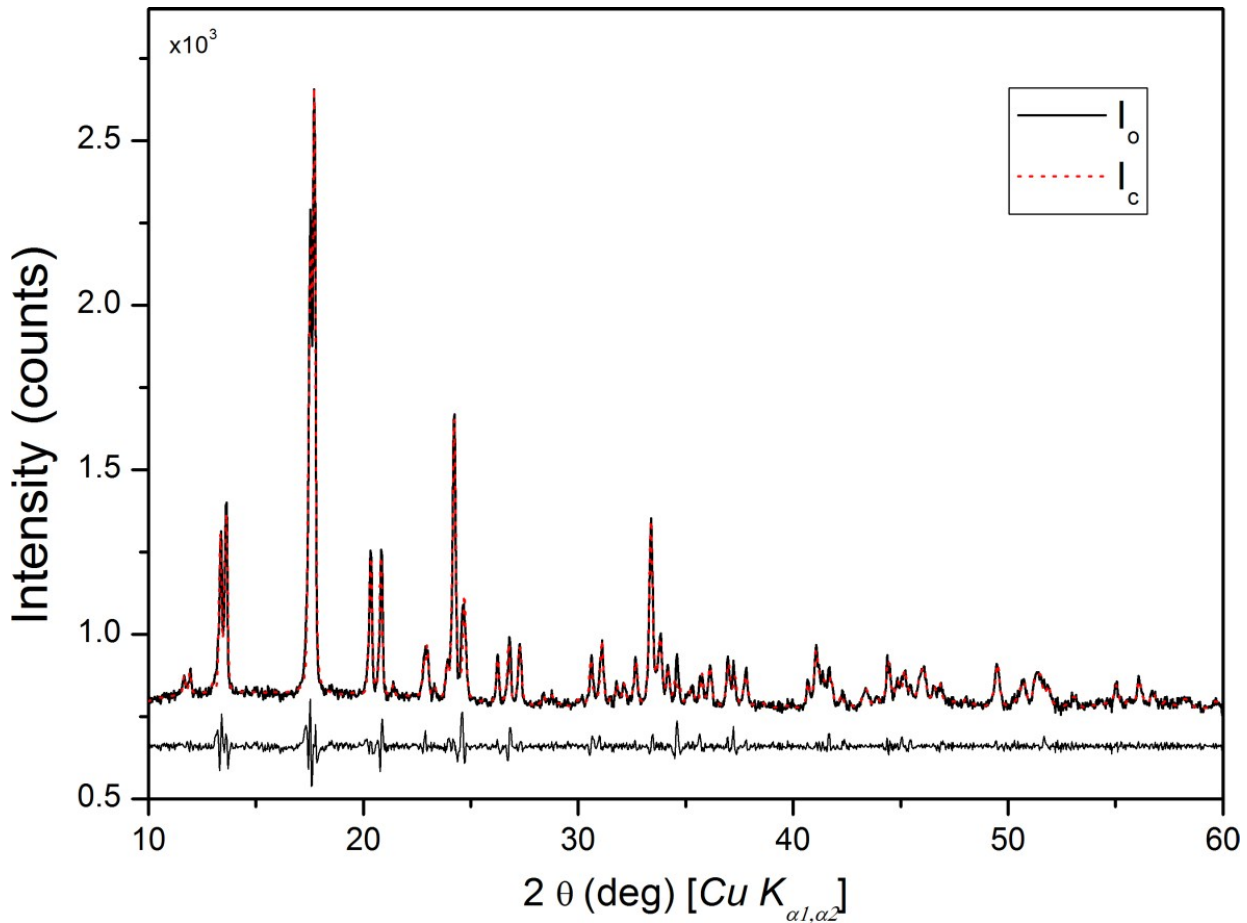


Figure S1. The results of the Le Bail refinement for bnMn powder at room temperature. The crystal system monoclinic, space group *Cc*. The final agreement R factors for the profile: R_p :0.010; wR_p =0.017; $GooF$ =0.015; The refined lattice parameters: $a=9.569(2)\text{\AA}$, $b=15.303(2)\text{\AA}$, $c=13.711(2)\text{\AA}$. I_o and I_c denote observed and calculated intensities, respectively. The difference plot is given at the bottom. Jana2006 was used for the calculations [Petricek, V., Dusek, M. & Palatinus, L. (2014). *Z. Kristallogr.* 229(5), 345-352].

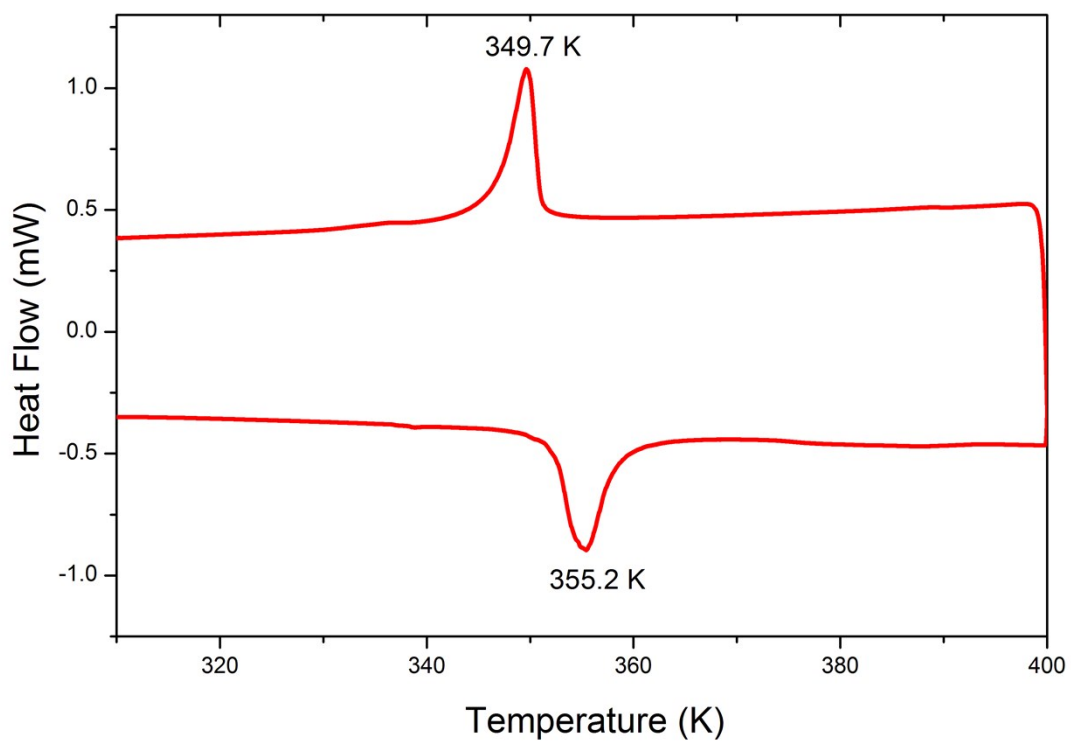


Figure S2. DSC traces for bnMn in heating and cooling mode.

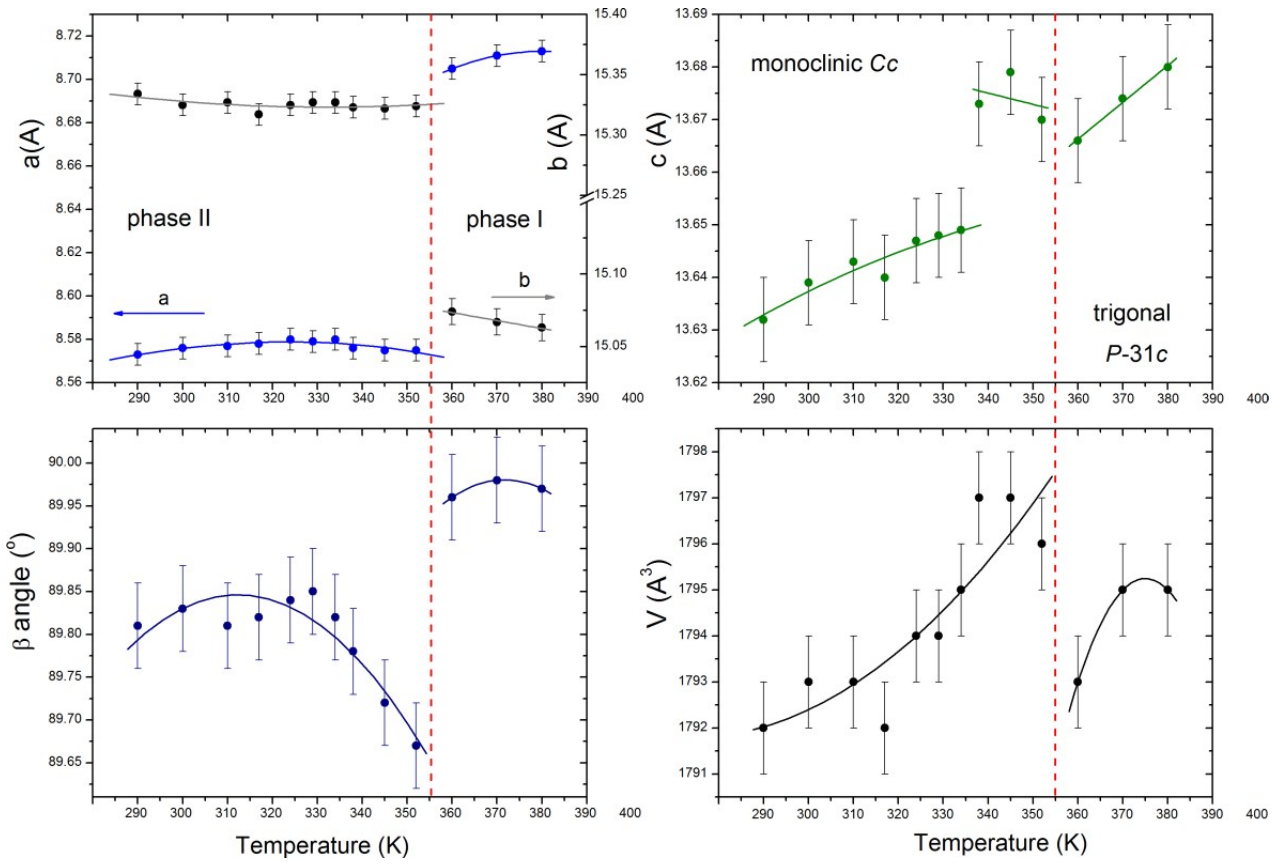


Figure S3. Temperature evolution of monoclinic lattice parameters in bnMn during heating. The lines are the guides for eyes.

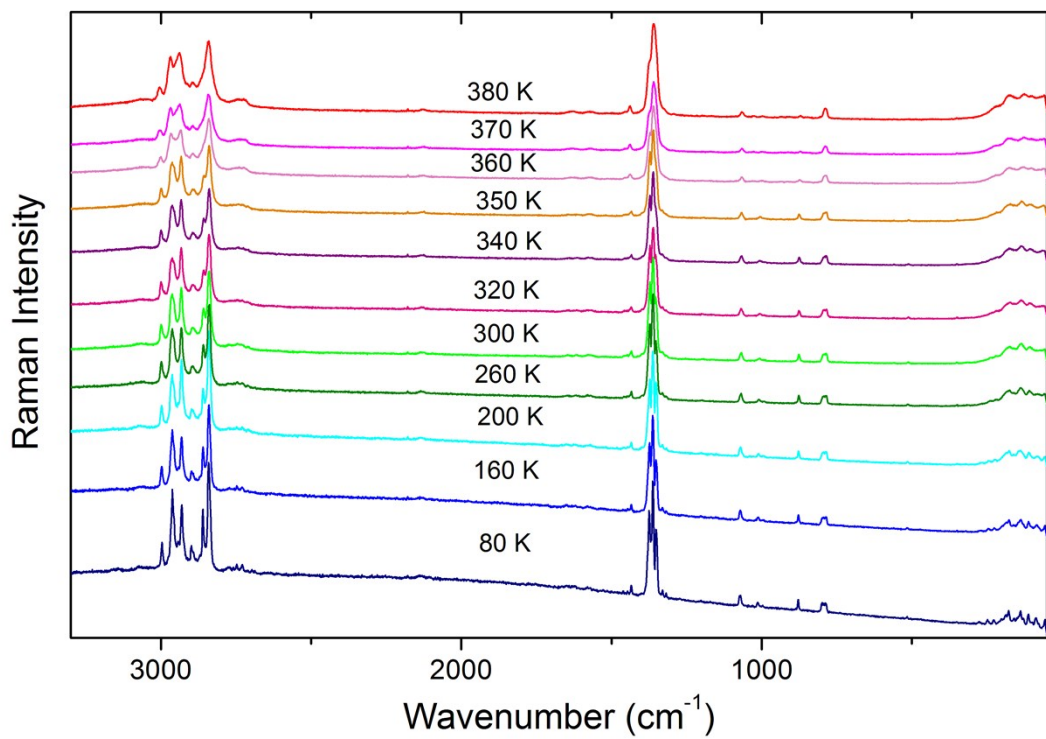


Figure S4. Raman spectra of bnMn recorded at various temperatures.

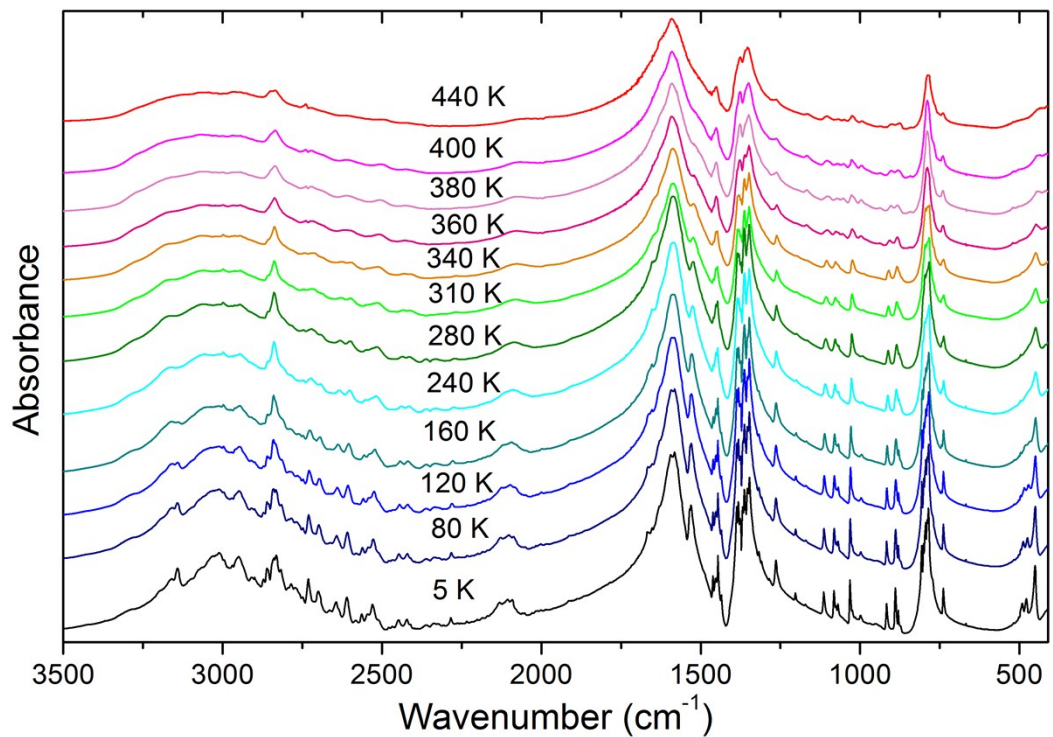


Figure S5. IR spectra of bnMn recorded at various temperatures in the 400-3500 cm⁻¹ range.

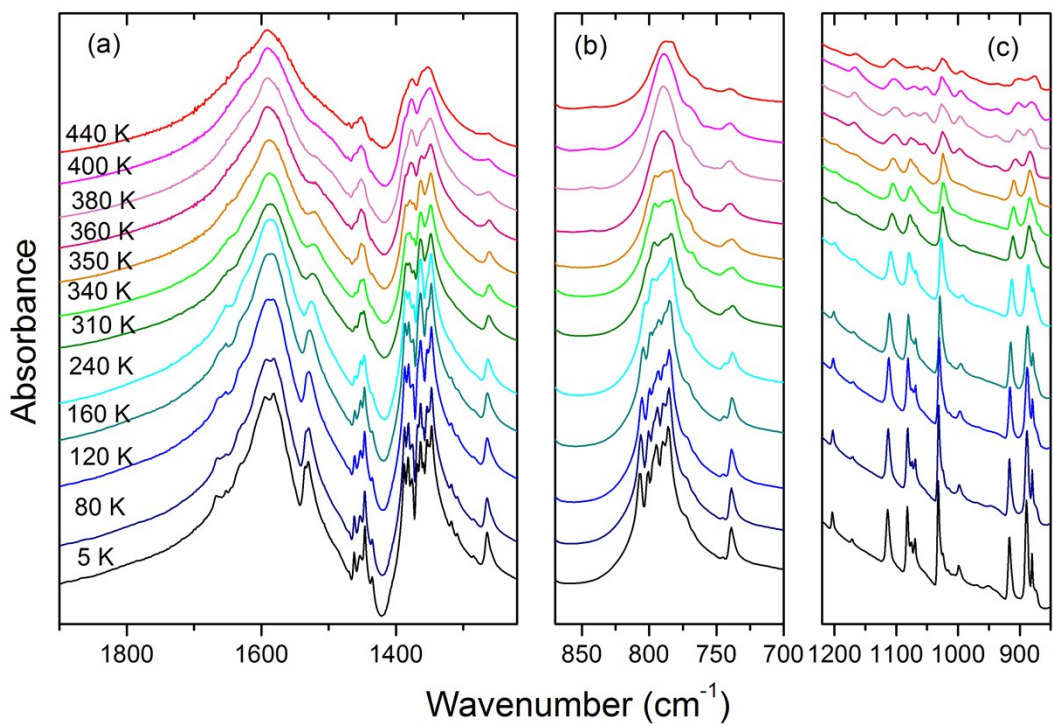


Figure S6. Detail of the IR spectra corresponding to the spectral ranges 1220-1900, 700-870 and 850-1220 cm^{-1} at different temperatures.

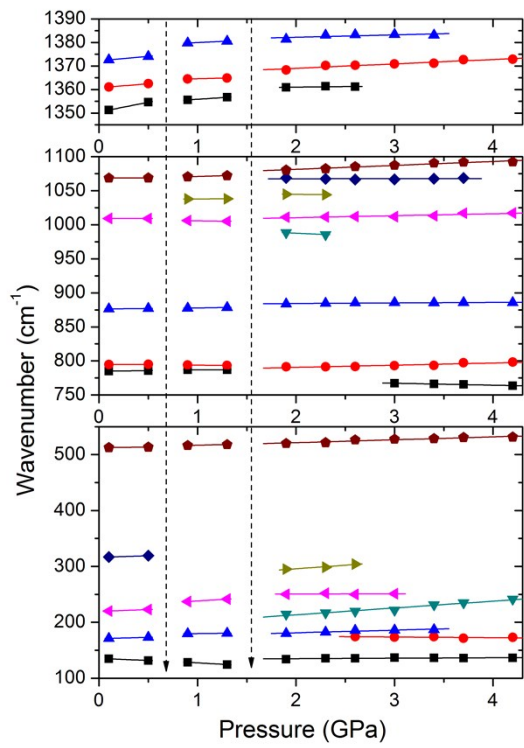


Figure S7. Wavenumber vs. pressure plots of the Raman modes observed in bnMn crystal for compression experiment. The solid lines are linear fits on the data to $\omega(P) = \omega_0 + \alpha P$. Vertical lines show the pressures at which structural phase transitions occur.

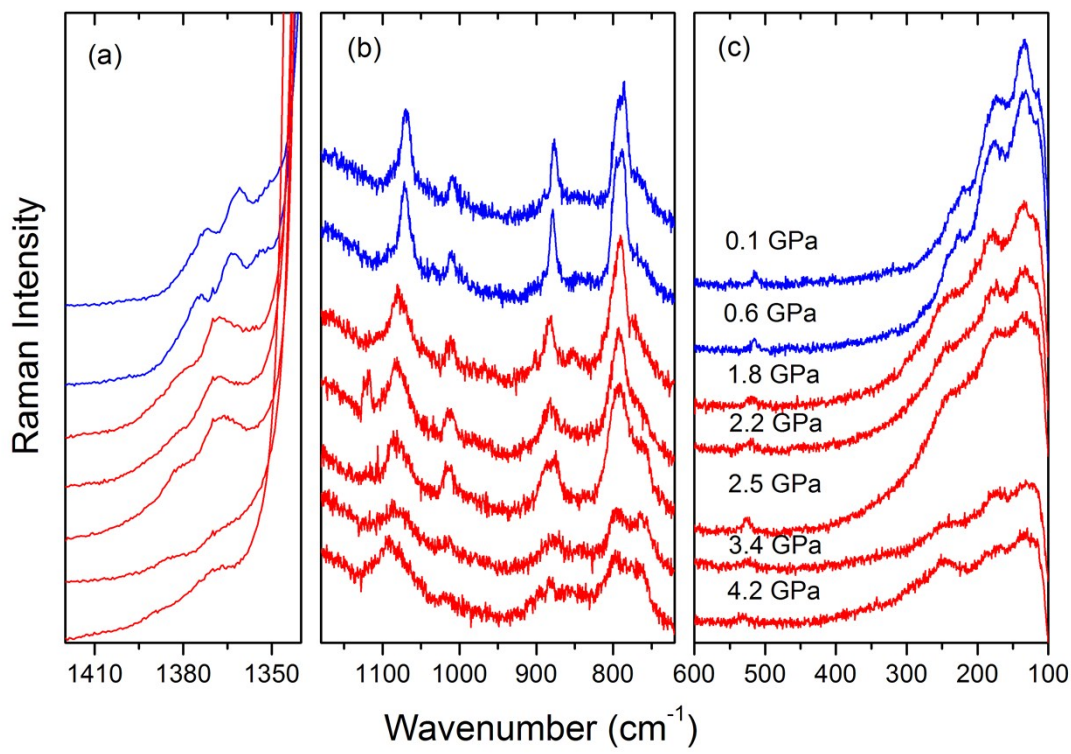


Figure S8. Raman spectra of bnMn recorded during decompression experiment.